Determination of earthquake focal depths and source time functions in central Asia using teleseismic *P* waveforms

Risheng Chu,[1,2] Lupei Zhu,[1] and Don V. Helmberger[2]

Received 5 June 2009; revised 14 July 2009; accepted 7 August 2009; published 12 September 2009.

[1] We developed a new method to determine earthquake source time functions and focal depths. It uses theoretical Green's function and a time-domain deconvolution with positivity constraint to estimate the source time function from the teleseismic *P* waveforms. The earthquake focal depth is also determined in the process by using the time separations of the direct *P* and depth phases. We applied this method to 606 earthquakes between 1990 and 2005 in Central Asia. The results show that the Centroid Moment Tensor solutions, which are routinely computed for earthquake larger than *M*5.0 globally using very long period body and surface waves, systematically overestimated the source depths and durations, especially for shallow events. Away from the subduction zone, most of the 606 earthquakes occurred within the top 20 km of crust. This shallow distribution of earthquakes suggests a high geotherm and a weak ductile lower crust in the region. **Citation:** Chu, R., L. Zhu, and D. V. Helmberger (2009), Determination of earthquake focal depths and source time functions in central Asia using teleseismic *P* waveforms, *Geophys. Res. Lett.*, *36*, L17317, doi:10.1029/2009GL039494.

1. Introduction

[2] Each seismogram is a convolution of instrument response, seismic wave propagation effect, earthquake radiation pattern, and earthquake source time function. Among them the instrument response is known and can be removed at the time of data preparation. The earthquake radiation pattern is calculated from its focal mechanism. The propagation effect is expressed in terms of the Green's functions, which are determined from Earth's velocity structure and the earthquake depth. The source time function is related to earthquake rupture processes. For small earthquakes, the source durations are very small and the source time functions are simple. A triangle or trapezoid function is often used to approximate the source time function. For events larger than $\sim M6.0$, the source time functions are much more complicated and need to be determined case by case.

[3] In order to separate the source time function and propagation effect, several deconvolution techniques have been developed. One direct method is the homomorphic deconvolution, which uses a linear operator to transform the convolution in the time domain to addition in the quefrency domain [*Ulrych*, 1971]. The source time function is the low-pass filtering result of the complex cepstrum. This technique has difficulty in phase unwrapping in the presence of additive noise [*Jin and Rogers*, 1983]. Another commonly used technique is the empirical Green's function method [e.g., *Dreger*, 1994]. It uses seismograms from aftershocks that have similar focal mechanisms and locations as the main-shock as the Green's functions. Deconvolution of the main-shock seismograms with the empirical Green's functions removes the effects of the path and site response. This technique requires that the corner frequency of aftershock be much higher than that of the main-shock. Usually, the magnitude of the aftershock should be two magnitudes smaller than the magnitude of the main-shock. One of the drawbacks is that the empirical Green's functions are easily affected by noise because the aftershock seismograms have much smaller amplitudes. *Brudzinski and Chen* [2000] used teleseismic *P* waveforms in similar azimuths as the effective source time function for modeling waveforms at regional distances. Because of the depth phases, their method only works for deep events, or the source time function will be contaminated by the depth phases.

[4] In this paper, we developed a new technique to estimate the source time function and to determine earthquake focal depth using teleseismic *P* waveforms. We used theoretical Green's functions to estimate source time function. Earthquake depth is also determined using the separations between the direct *P* and depth phases in the process. We applied the method to earthquakes in central Asia (Figure 1) and compared the results with those of the Centroid Moment Tensor (CMT) solutions. The tectonic implications of earthquake depth distribution in the region were also discussed.

2. Method

[5] We used teleseismic *P* waveforms ($30^\circ - 90^\circ$) to determine earthquake source time function and depth. At this distance range, seismic rays travel mostly in the lower mantle and are free of the complexities caused by reflection or refraction in the upper mantle and near the core-mantle boundary. The *P*-wave seismograms consist of the direct *P* wave and the depth phases *pP* and *sP*. The differential travel times between *P*-*pP* and *P*-*sP* are controlled by the event depth and can be used to estimate the earthquake focal depth. We computed the theoretical Green's functions using the generalized ray method [*Helmberger*, 1983]. The global average Earth velocity model IASPEI91 [*Kennett and Engdahl*, 1991] was used, with its 30-km-thick crust replaced by a 45-km-thick crust to account for the thick crust in the region.

[6] Earthquake source time functions were obtained by deconvolving the vertical component of teleseismic *P*-wave

[1]Department of Earth and Atmospheric Sciences, Saint Louis University, Saint Louis, Missouri, USA.
[2]Seismological Laboratory, California Institute of Technology, Pasadena, California, USA.

0094-8276/09/2009GL039494$05.00

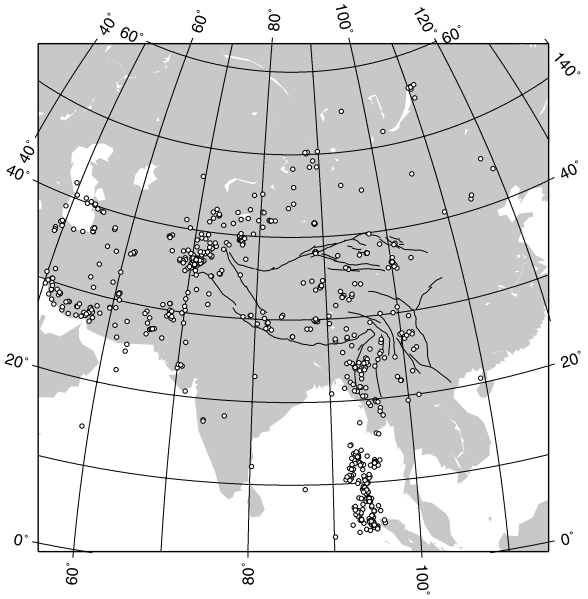

Figure 1. Locations of 606 earthquakes (circles) with magnitude $M \geq 5$ between 1990 and 2005 analyzed in this study. Lines represent major faults around the Tibetan plateau.

waveforms with the impulse-response (source-free) synthetic seismograms. Both the data and synthetic seismograms were band-pass filtered between 0.02 Hz and 1 Hz. We used a time domain iterative deconvolution technique [*Kikuchi and Kanamori*, 1982]. Because source time functions are always positive, we added a positivity constraint to the deconvolution algorithm. For each event, we stacked all the source time functions obtained from stations in different directions to obtain the average source time function.

[7] In deconvolution, we used a time window centered at the direct *P* with its length about twice of the estimated duration of the source time function. For deep earthquakes, the separations between the direct *P* and depth phases are large enough so that the depth phases do not interfere with the source time function in the direct *P* wave. Figure 2a shows teleseismic vertical displacements from a Mb 5.9 earthquake in northern Sumatra, Indonesia, on 09/05, 2003. The CMT depth of the event is 125 km. The depth phase *pP* is at about 30 s after the direct *P* and the shape of the direct *P* wave is essentially a band-pass filtered version of the source time function. After deconvolving the direct *P*-wave waveforms with the corresponding source-free synthetic seismograms (red traces in Figure 2), we obtained the source time function with a duration of about 2 s. We then removed the source time function from the observed *P* waveforms by deconvolution. The source-free *P* waveforms (black traces in the middle column) show sharper direct *P*, *pP*, and *sP* phases than the original waveforms which allowed us to fine-tune the source depth to 120 km in order to match the separation between *P* and *pP*. In this case, error in the initial source depth used to compute the synthetic seismograms does not affect the source time function estimation since all depth phases are beyond the deconvolution time window.

[8] For shallow events, however, their depth phases are often close to or within the source duration. Figure 2b shows teleseismic vertical displacements from a Mb 5.6 earthquake near the India-Bangladesh border region on 07/26, 2003. The CMT depth is at 15 km. The first 5-s *P* waveforms are controlled by the direct *P* and the depth phases *pP* and *sP*. The theoretical Green's functions in the deconvolution window change with the source depth. In this case, we estimated the source time function and source depth iteratively, starting at its CMT depth and repeated the deconvolution procedure by adjusting the source depth until the source-free *P* waveforms match the source-free synthetic seismograms (Figure 2). For this earthquake, we found that the source duration was about 3.0 s and a source depth of 12 km gave the best waveform fit.

3. Data and Results

[9] We applied the method to earthquakes with distances less than 30° from the center of the Tibetan Plateau (85°E, 33°N). This area covers most of Central Asia. Using the CMT catalog, we found 929 earthquakes between January 1990 and February 2005 with magnitudes larger than *M*5.0. We downloaded their teleseismic waveforms recorded by Global Seismographic Network (GSN) stations from the IRIS data management center. We removed instrument responses and filtered the waveform using a bandpass filter with corner frequencies of 0.02 Hz and 1.0 Hz.

[10] Our first step was to verify the CMT focal mechanisms by comparing the observed teleseismic *P* and *S* waveforms with synthetic seismograms predicted by the CMT solution. When computing synthetics, we simply used the CMT depth and a triangle or trapezoid as the source time function. If the synthetics match the observations in shape and polarity in general, we considered the solution to be correct. In total, we found 606 events with good focal mechanisms (Figure 1). Other events' CMT solutions predict wrong *P* or *S* waveform polarities at some teleseismic stations and were not used in the next step.

[11] We obtained source time functions and depths for all 606 earthquakes using the procedure described in the previous section. We required that each event had at least one identifiable depth phase and the source-free waveforms matched the predictions. Because a perturbation of 1 km in source depth will produce a 0.2 to 0.3 s change in the separation between the direct *P* and depth phases, which is easily noticeable in the waveform fits, we estimated the uncertainties of depths to be less than 1 km for most events. Figure 3 shows comparisons of event depths and source durations with those from the CMT catalog. It is clear that the re-determined event depths are generally shallower than the CMT depths, especially for shallow events. The differences between the two depths can be as large as 100 km. In the CMT catalog, earthquake depths are estimated by minimizing the waveform misfits between observed and synthetic body and surface waves at very long period (longer than 45 s for body waves, 135 s for surface waves) [*Dziewonski et al.*, 1981; *Ekström and Dziewonski*, 1985]. Because long period waves are not sensitive to event depths, the CMT depths are not well constrained. In addition, the CMT depths are restricted to be larger than 10 km in order to minimize instabilities of the moment tensor inversion at very shallow depths [*Arvidsson and Ekström*, 1998]. We used the separations between the direct *P* and the depth

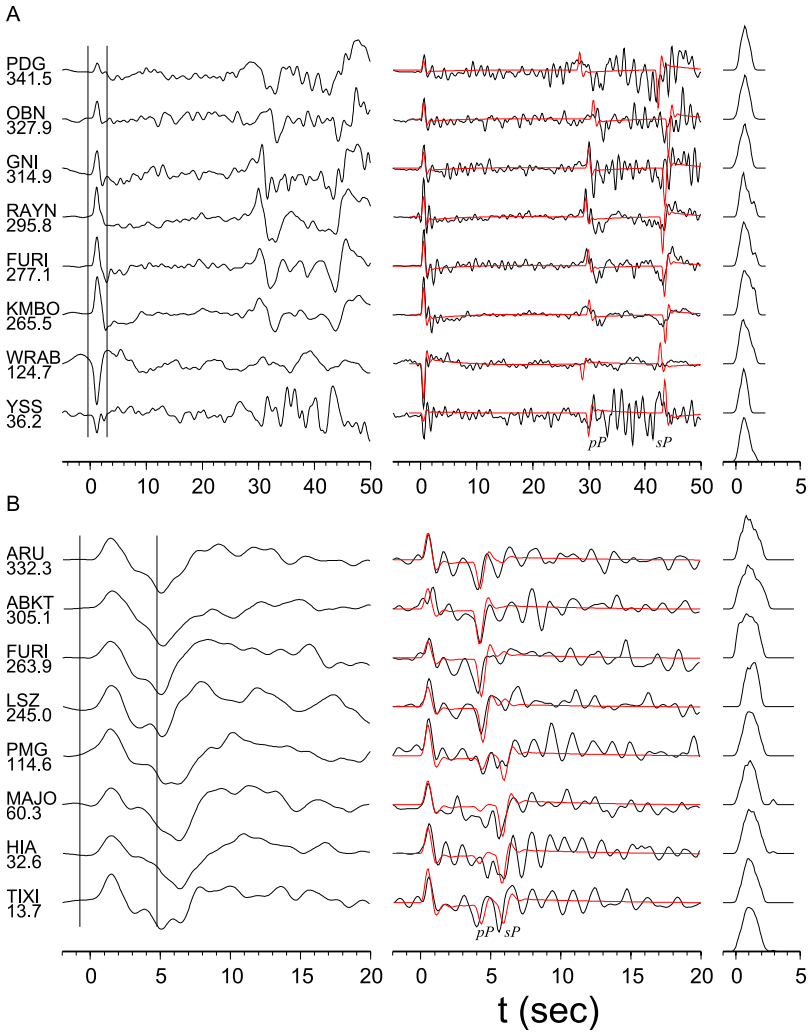

Figure 2. (a) Source time function and depth estimation for a Mb 5.9 earthquake in Indonesia on 09/05/2003. The vertical components of teleseismic *P* waveforms shown in the left column are deconvolved from the source-free synthetic seismograms (red-color traces) in the middle column to produce the source time functions shown in the right column. The two vertical lines indicate the time window for deconvolution. The numbers beneath the station names are station azimuths in degrees. The averaged source time function is shown at the bottom in the right column. It is removed from the data by deconvolution to produce the source-free *P* waveforms shown as black traces in the middle column. (b) The same procedure for a shallow earthquake near the India-Bangladesh border region on 07/26/2003.

phases at teleseismic distances to determine the event focal depths which are more reliable.

[12] We also compared our focal depths with those in the EHB Bulletin (Figure 3) which uses teleseismic depth phase arrival times to constrain earthquake depths [*Engdahl et al.*, 1998; *International Seismological Centre*, 2009]. Our depths agree with the EHB depths much better than with the CMT depths, with a smaller scattering and no system-

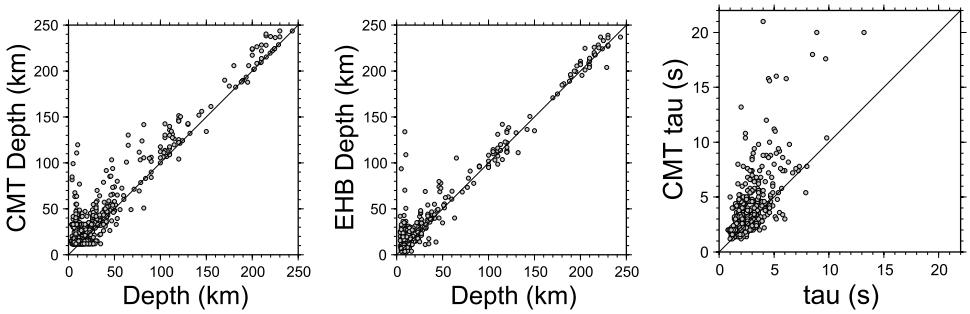

Figure 3. Comparisons of focal depths and source durations τ determined in this study with the CMT solutions and the depths in the EHB Bulletin.

atical bias for events deeper than 20 km. We noted a few events that EHB located at much greater depths (>50 km) than our depths (<10 km). We checked their teleseismic waveforms and confirmed that they were indeed shallow, see Figure S1 of the auxiliary material.[1] The deeper EHB depths are likely to be caused by misidentification of depth phases in the seismic station reports.

[13] Based on the re-determined focal depths, more the two thirds of the 606 earthquakes occurred within the top 20 km of crust. This shallow distribution of earthquakes suggests a high geotherm and a weak ductile lower crust in the region [e.g., *Chen and Molnar*, 1983; *Zhao and Helmberger*, 1991]. All earthquakes deeper than 100 km are associated with the current subduction zones along the Burma-Indonesia arc and in the Pamir-Hindu Kush region. Outside the subduction zones, we only found two earthquakes at the intermediate depth range, one in southern Tibet (06/09/1996, Mb 5.2 and depth 84 km) and one in southern Iran (06/10/1998, Mb 5.4 and depth 82 km). Similar intermediate-depth earthquakes were found before beneath the Himalayas and southern Tibet [*Molnar and Chen*, 1983; *Chen et al.*, 1981; *Chen*, 1988; *Zhu and Helmberger*, 1996]. The origin of these intermediate-depth earthquakes has been debated. *Zhu and Helmberger* [1996] and *Chen and Yang* [2004] suggested that they occurred in the mantle part of lithosphere as a result of increase in lithospheric strength from the ductile lower crust to brittle uppermost mantle due to compositional change. Others [e.g., *Priestley et al.*, 2008] argued that they occurred at the base of Tibetan lower crust due to subduction of the Indian slab. The intermediate-depth earthquake in southern Iran is most likely related to the collision between the Arabian plate and Eurasia.

[14] The CMT catalog also provides source durations. The durations are not determined from the CMT inversion but estimated from the moment magnitude using empirical relationships [*Helffrich*, 1997]. Figure 3 shows that the actual source durations are smaller than those listed in the CMT catalog.

4. Conclusions

[15] In summary, we developed a new method to determine earthquake source time functions and focal depths. It uses theoretical Green's function and a time-domain deconvolution with positivity constraint to estimate the source time function from the teleseismic *P* waveforms. The earthquake focal depth is also determined in the process by using the time separations of the direct *P* and depth phases. We applied this method to 606 earthquakes in Central Asia. The results show that the CMT solutions, routinely obtained using very long period body and surface waves, systematically over-estimated the source depths and durations, especially for shallow events. Away from the subduction zone, most of the 606 earthquakes occurred within the top 20 km of crust. This shallow distribution of earthquakes suggests a high geotherm and a weak ductile lower crust in the region.

[16] **Acknowledgments.** We are grateful to Alex Hutko and another GRL reviewer for their constructive comments that helped us to improve the manuscript. All waveform data used in this study were obtained from IRIS Data Management Center. This material is based upon work supported by the NSF under grant EAR-0439992. Risheng Chu was also partially supported by NSF grant EAR-0337491. This is contribution 10025 of the Caltech Seismological Laboratory.

References

Arvidsson, R., and G. Ekström (1998), Global CMT analysis of moderate earthquakes, $M_w \geq 4.5$, using intermediate-period surface waves, *Bull. Seismol. Soc. Am.*, *88*, 1003–1013.

Brudzinski, M. R., and W.-P. Chen (2000), Variation in *P* wave speeds and outboard earthquakes: Evidence for a petrologic anomaly in the mantle transition zone, *J. Geophys. Res.*, *105*, 21,661–21,682.

Chen, W.-P. (1988), A brief update on the focal depths of intracontinental earthquakes and their correlation with heat flow and tectonic age, *Seismol. Res. Lett.*, *59*, 263–272.

Chen, W.-P., and P. Molnar (1983), Focal depths of intracontinental and intraplate earthquakes and their implications for the thermal and mechanical properties of the lithosphere, *J. Geophys. Res.*, *88*, 4183–4214.

Chen, W.-P., and Z. Yang (2004), Earthquakes beneath the Himalayas and Tibet: Evidence for strong lithospheric mantle, *Science*, *304*, 1949–1952, doi:10.1126/science.1097324.

Chen, W.-P., J. L. Nábelek, T. J. Fitch, and P. Molnar (1981), An intermediate depth earthquake beneath Tibet: Source characteristics of the event of September 14, 1976, *J. Geophys. Res.*, *86*, 2863–2876.

Dreger, D. S. (1994), Empirical Green's function study of the January 17, 1994 Northridge, California earthquake, *Geophys. Res. Lett.*, *21*, 2633–2636.

Dziewonski, A. M., T.-A. Chou, and J. H. Woodhouse (1981), Determination of earthquake source parameters from waveform data for studies of global and regional seismicity, *J. Geophys. Res.*, *86*, 2825–2852.

Ekström, G., and A. M. Dziewonski (1985), Centroid-moment tensor solutions for 35 earthquakes in western North America (1977–1983), *Bull. Seismol. Soc. Am.*, *75*, 23–39.

Engdahl, E. R., R. van der Hilst, and R. Buland (1998), Global teleseismic earthquake relocation with improved travel times and procedures for depth determination, *Bull. Seismol. Soc. Am.*, *88*, 722–743.

Helffrich, G. R. (1997), How good are routinely determined focal mechanisms? Empirical statistics based on a comparison of Harvard, USGS and ERI moment tensors, *Geophys. J. Int.*, *131*, 741–750.

Helmberger, D. V. (1983), Theory and application of synthetic seismograms, in *Earthquakes: Observation, Theory and Interpretation*, pp. 174–222, Soc. Ital. di Fis., Bolgna, Italy.

International Seismological Centre (2009), EHB Bulletin, www.isc.ac.uk, Int. Seismol. Cent., Thatcham, UK.

Jin, D. J., and J. R. Rogers (1983), Homomorphic deconvolution, *Geophysics*, *48*, 1014–1016.

Kennett, B. L. N., and E. R. Engdahl (1991), Travel times for global earthquake location and phase identification, *Geophys. J. Int.*, *105*, 429–465.

Kikuchi, M., and H. Kanamori (1982), Inversion of complex body waves, *Bull. Seismol. Soc. Am.*, *72*, 491–506.

Molnar, P., and W.-P. Chen (1983), Focal depths and fault plane solutions of earthquakes under the Tibetan Plateau, *J. Geophys. Res.*, *88*, 1180–1196.

Priestley, K., J. Jackson, and D. McKenzie (2008), Lithospheric structure and deep earthquakes beneath India, the Himalaya and southern Tibet, *Geophys. J. Int.*, *172*, 345–362.

Ulrych, T. J. (1971), Application of homomorphic deconvolution to seismology, *Geophysics*, *36*, 650–660.

Zhao, L. S., and D. V. Helmberger (1991), Geophysical implication from relocation of Tibetan earthquakes; hot lithosphere, *Geophys. Res. Lett.*, *18*, 1070–1084.

Zhu, L., and D. V. Helmberger (1996), Intermediate depth earthquakes beneath the India-Tibet collision zone, *Geophys. Res. Lett.*, *23*, 435–438, doi:10.1029/96GL00385.

R. Chu and D. V. Helmberger, Seismological Laboratory, California Institute of Technology, Pasadena, CA 91125, USA. (chur@gps.caltech.edu)

L. Zhu, Department of Earth and Atmospheric Sciences, Saint Louis University, Saint Louis, MO 63108, USA.

[1] Auxiliary material data sets are available at ftp://ftp.agu.org/apend/gl/2009gl039494. Other auxiliary material files are in the HTML.